7(c). Microbial mat features in mudstones of the Mesoproterozoic Somanpalli Group, Pranhita-Godavari Basin, India

S.P. Deb, J. Schieber and A.K. Chaudhuri

The Pranhita-Godavari Basin is located in the northeastern portion of peninsular India (Fig. 7(c)-1) and contains several kilometers of Proterozoic sediments (Chaudhuri et al., 1999, 2002). A mudstone-shale dominated succession of Mesoproterozoic age developed around Somanpalli along the northeastern margin of the Pranhita-Godavari valley adjoining the Bastar craton (Fig. 7(c)-1), is known as the Somanpalli Group (Saha and Gosh, 1998).

Recent stratigraphic analysis of the Somanpalli Group indicates that the lowest formation of the group, the Somnur Formation, comprises a thick shelf sequence of cross-stratified and planar-stratified sandstone, sandstone-mudstone heterolithic intervals, and shale, approximately 1000 m thick. The Somnur Formation grades upwards into the Tarur Nala Formation, an approximately 1000 m thick succession dominated by mudstones and shales, minor carbonates, and very minor amounts of fine-grained dark sandstone. The lower part of the Tarur Nala Formation is dominated by black to steel grey mudstone and shale (Sample No.S-3-3A), whereas its upper part comprises a very persistent striped-shale with red and light buff banding (Rest House Shale; samples SGH 1 &2). A few lenses of coarse-grained to gritty sandstone occur at the top of the Rest House Shale, probably the fill of erosive submarine channels (Sample BJ 07/03). The sandstone lenses represent the coarsest grade of siliciclastics, constitute a minor fraction of the succession, and may be an indicator of falling sea level towards the end of Tarur Nala deposition.

The Tarur Nala Formation is overlain by the Bodela Vagu limestone, interpreted as a slope-basin deposit (Fig. 7(c)-2). The Bodela grades upwards into the Kopela Shale, a turbidite-pelagite deposit with very minor amounts of sandstone. The Kopela Shale is dominated by massive and thinly laminated black shale (Sample Nos. 8E/95 & 4/5). The Somanpalli Group is unconformably overlain by the Po Gutta Sandstone. This unconformity most likely denotes a major hiatus. The Po Gutta Sandstone is a formation of the Neoproterozoic Albaka Group.

Figure 7(c)-3 (images A-D) illustrates carbonaceous shales from the lower portion of the Tarur Nala Formation. A characteristic feature of these shales is that they contain carbonaceous fragments (1mm or less in size) that look variably degraded when compared with likely microbial mat fragments from other units in the Somanpalli Group (Figs. 7(c)-4 and 7(c)-6). Whether these fragments are indeed degraded and redposited microbial mat fragments is difficult to ascertain, but they do appear to be fragments that were deposited in a soft and pliable state and contained carbonaceous laminae (Fig. 7(c)-3 B). These shales resemble gray shales with carbonaceous streaks and lumps that were

In: *Atlas of microbial mat features preserved within the clastic rock record*, Schieber, J., Bose, P.K., Eriksson, P.G., Banerjee, S., Sarkar, S., Altermann, W., and Catuneau, O., (Eds.), Elsevier, p. 171-180. (2007)

described from distal shale facies in the eastern Belt Basin (Schieber, 1989). In the latter example carbonaceous streaks and lumps were interpreted as redeposited microbial mat fragments because of lateral association with shale facies that contained benthic microbial mats (Schieber, 1986).

Figure 7(c)-4 illustrates shales from the middle portion of the Tarur Nala Formation. The most striking feature about these shales is their banded or striped nature (Fig. 7(c)-4A). The shales consist of gray clay dominated layers that alternate with reddish layers that show a faint wavy internal lamination. When viewed in detail, it is obvious that the reddish colour is due to secondary formation of iron oxides (Fig. 7(c)-4B, -4C, -4D & -4E), probably derived from oxidation of finely disseminated pyrite during weathering. The reddish layers also show more abundant and larger silt grains and wavy-crinkly internal laminae (Fig. 7(c)-4D, -4E & -4F). Texturally, these shales are a very close match to striped shales from the Mid-Proterozoic Belt Supergroup (Schieber, 1986; compare with Figure 5-3 of this book). The latter were interpreted as the deposits of benthic microbial mats (carbonaceous pyritic layers) whose accumulation was intermittently interrupted by rapid deposition of storm-derived mud drapes (gray clay layers). By direct comparison with its Belt Basin counterpart (Schieber, 1986), the reddish layers in the striped shales from the Tarur Nala Formation are interpreted as the weathered equivalents of wavy laminated carbonaceous-pyritic layers in Belt Basin striped shales. Although in the Tarur Nala samples all of the original pyrite and carbonaceous matter have been oxidized, the textural details, such as wavy-crinkly internal lamination, silt enrichment, and sharp contacts between gray and red layers (Fig. 7(c)-4E) are the same as in the Belt Basin striped shales. Vertically and obliquely oriented embedded mica flakes in gray interbeds of the Tarur Nala striped shales (Fig. 7(c)-4G & -4H) suggest “hindered’ settling in a rapidly accumulating clay deposit. This supports the notion that, as in the Belt Basin example, these interlayers were event deposits, possibly due to storms or flood-related river plumes. Also, weathered and fully oxidized samples collected from Belt Basin outcrops look identical to the pictured samples of the Tarur Nala Formation (Schieber, 1985).

Figure 7(c)-5 illustrates shale fragments that occur in small lenses towards the top of the Tarur Nala Formation. Many of these fragments show wavy-crinkly carbonaceous laminae (Fig. 7(c)-5A, -5B, -5D, -5E & -5F), soft sediment deformation, and overfolding (Fig. 7(c)-5C) that in the context of other observations (Figs. 7(c)-4 and 7(c)-6) strongly suggest that these fragments were eroded from shales that were stabilized by benthic microbial mats. Non-carbonaceous shale fragments (Fig. 7(c)-5G & -5H) probably represent eroded gray interbeds and/or clay dominated shale facies from nearshore areas (e.g. Schieber, 1989).

In context, the samples from the Tarur Nala Formation suggest an overall shallowing-upwards trend. Distally deposited carbonaceous-streak-shales occur at the base of the succession (sample S-3-3A), pass upwards into striped shales deposited in an offshore

In: *Atlas of microbial mat features preserved within the clastic rock record*, Schieber, J., Bose, P.K., Eriksson, P.G., Banerjee, S., Sarkar, S., Altermann, W., and Catuneau, O., (Eds.), Elsevier, p. 171-180. (2007)

shelf setting (samples SGH 1 & 2), and erosive sand-filled channels with reworked mat fragments occur at the very top (sample BJ 07/03).

Shales from the Kopela Shale (Fig. 7(c)-2) are illustrated in Figures 7(c)-3 (images E – H) and 7(c)-6. Photomicrographs from the lower portion of the Kopela Shale show it to be a largely gray shale with abundant fine silt laminae (Fig. 7(c)-3E & -3F). In many instances the silt laminae show grading and may also form discernable silt-clay couplets (Fig. 7(c)-3F). Graded silt layers have sharp bases that may be erosional, and may also show evidence of loading of an unconsolidated surface (Fig. 7(c)-3G & -3H). In the context of observed sandy turbidites within this unit (Saha and Ghosh., 1998), these graded laminae and couplets are interpreted as fine-grained turbidites (Stow and Shanmugam, 1980). Figure 7(c)-6 shows photomicrographs from a massively bedded carbonaceous shale somewhat higher in the Kopela Shale succession (Fig. 7(c)-2). A characteristic feature of these shales is that they contain carbonaceous fragments (less than 1 mm to 10 mm in size) in a fine crystalline clay-silt matrix. The carbonaceous fragments can be very thin carbonaceous films that show overfolding and deformation (Fig. 7(c)-6A & -6B), or they are fragments of a shale with abundant wavy carbonaceous laminae (Fig. 7(c)-6C & -6D). These fragments have a high degree of textural similarity to redeposited microbial mat fragments in shales of the Mid-Proterozoic Belt Supergroup of Montana (Schieber, 1986, 1989). Overfolding of thin fragments during transport (Fig. 7(c)-6A & -6B) indicates that the material that constituted the thin carbonaceous films possessed considerable cohesive strength during transport t and deposition. Frayed edges of these fragments (Fig. 7(c)-6E & -6F) also attest to internal cohesion, and adherence of silt lenses during fragment transport (Fig. 7(c)-6E) suggests some binding material. All of these features are consistent with a microbial mat origin for the carbonaceous fragments. Larger fragments also show wavy-crinkly carbonaceous laminae of the same style as observed in benthic microbial mats from the Belt Supergroup (Schieber, 1986).

Figures and Captions: Chapter 7(c)

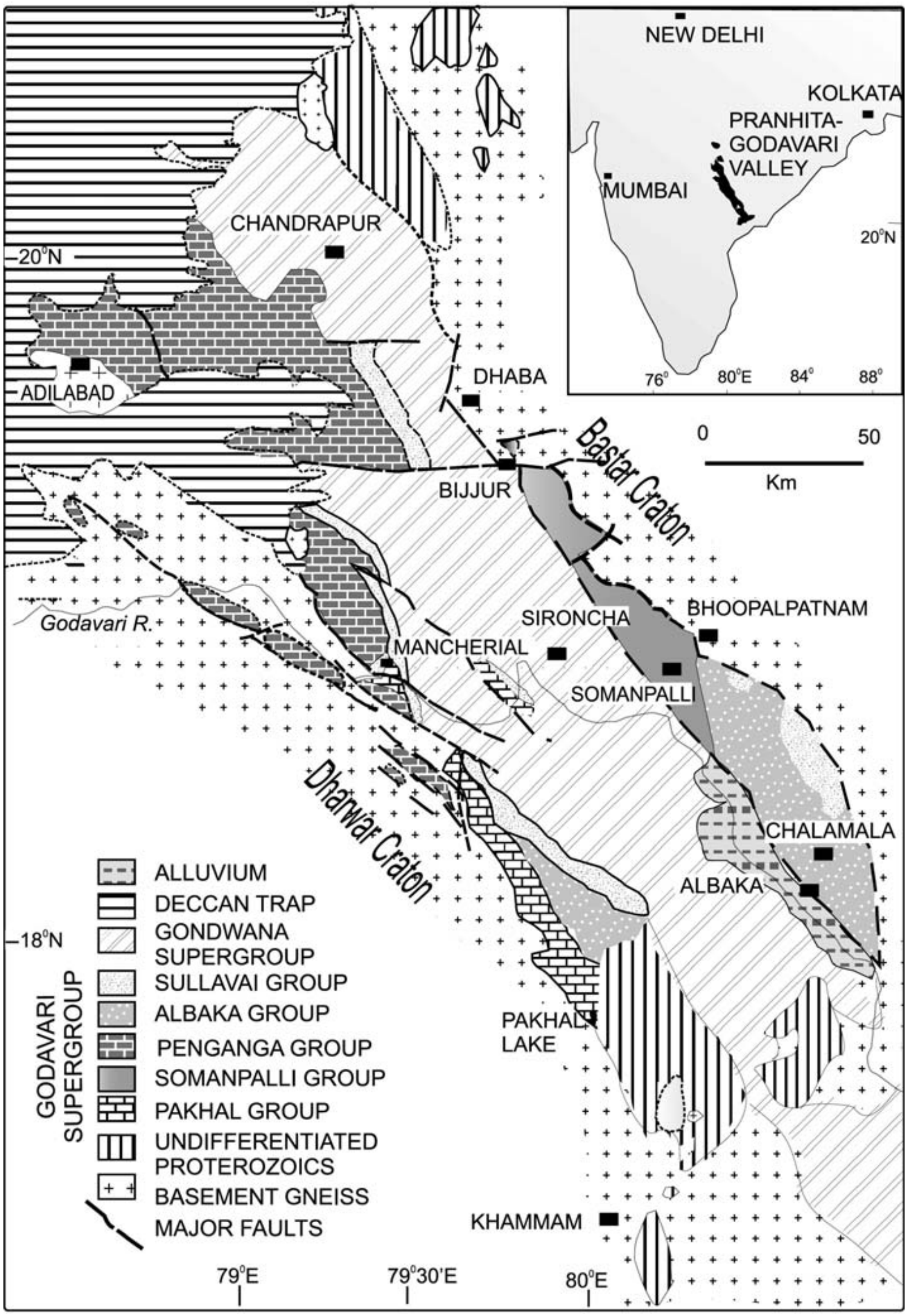

Fig. 7(c)-1: Schematic geologic map of the Pranhita-Godavari valley region. Outcrops of the Somanpalli Group occur to the right of the centre of the map.

In: *Atlas of microbial mat features preserved within the clastic rock record*, Schieber, J., Bose, P.K., Eriksson, P.G., Banerjee, S., Sarkar, S., Altermann, W., and Catuneau, O., (Eds.), Elsevier, p. 171-180. (2007)

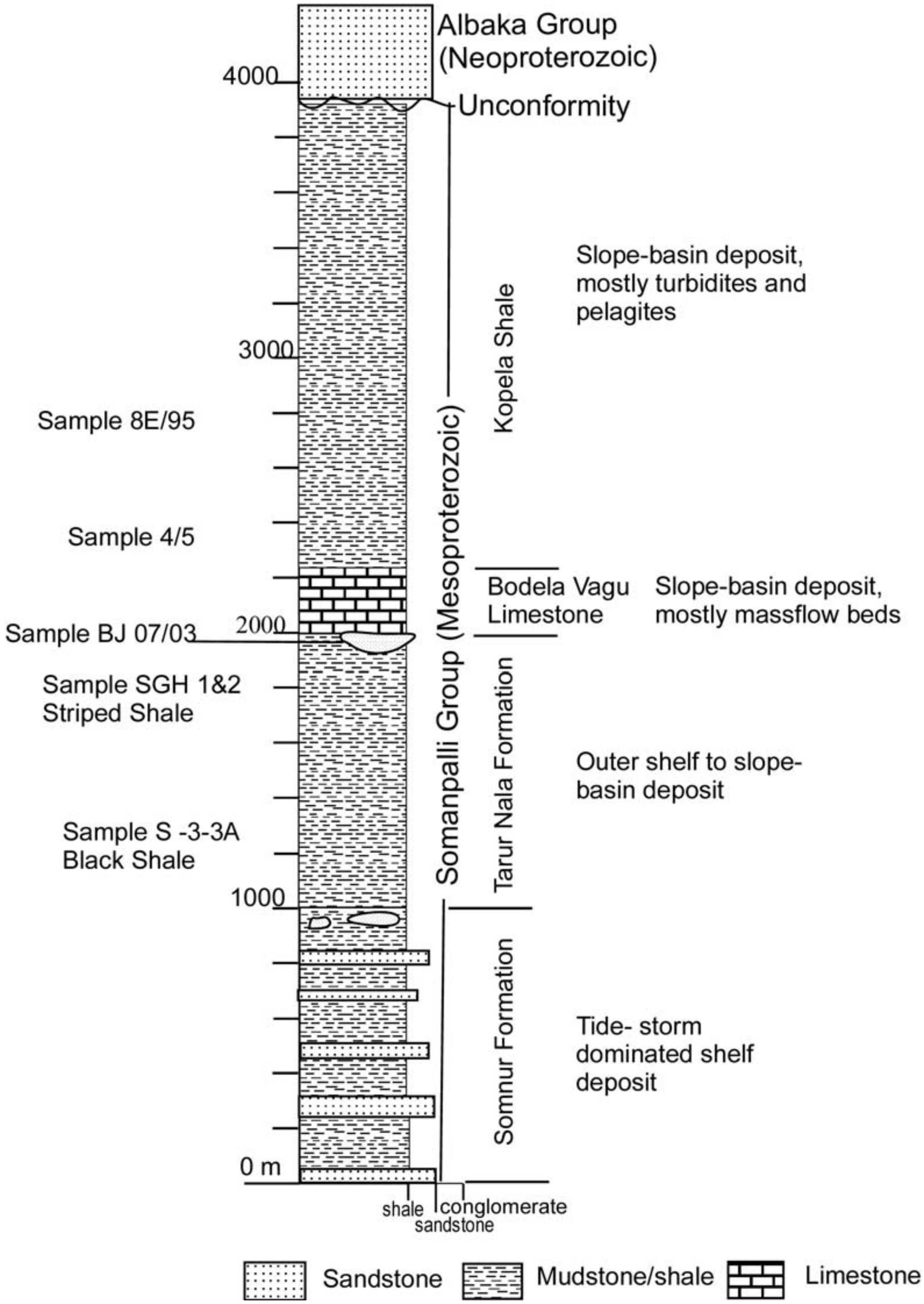

Fig. 7(c)-2: Simplified stratigraphic column of the Somanpalli Group with locations of described samples, and inferred depositional setting.

In: *Atlas of microbial mat features preserved within the clastic rock record*, Schieber, J., Bose, P.K., Eriksson, P.G., Banerjee, S., Sarkar, S., Altermann, W., and Catuneau, O., (Eds.), Elsevier, p. 171-180. (2007)

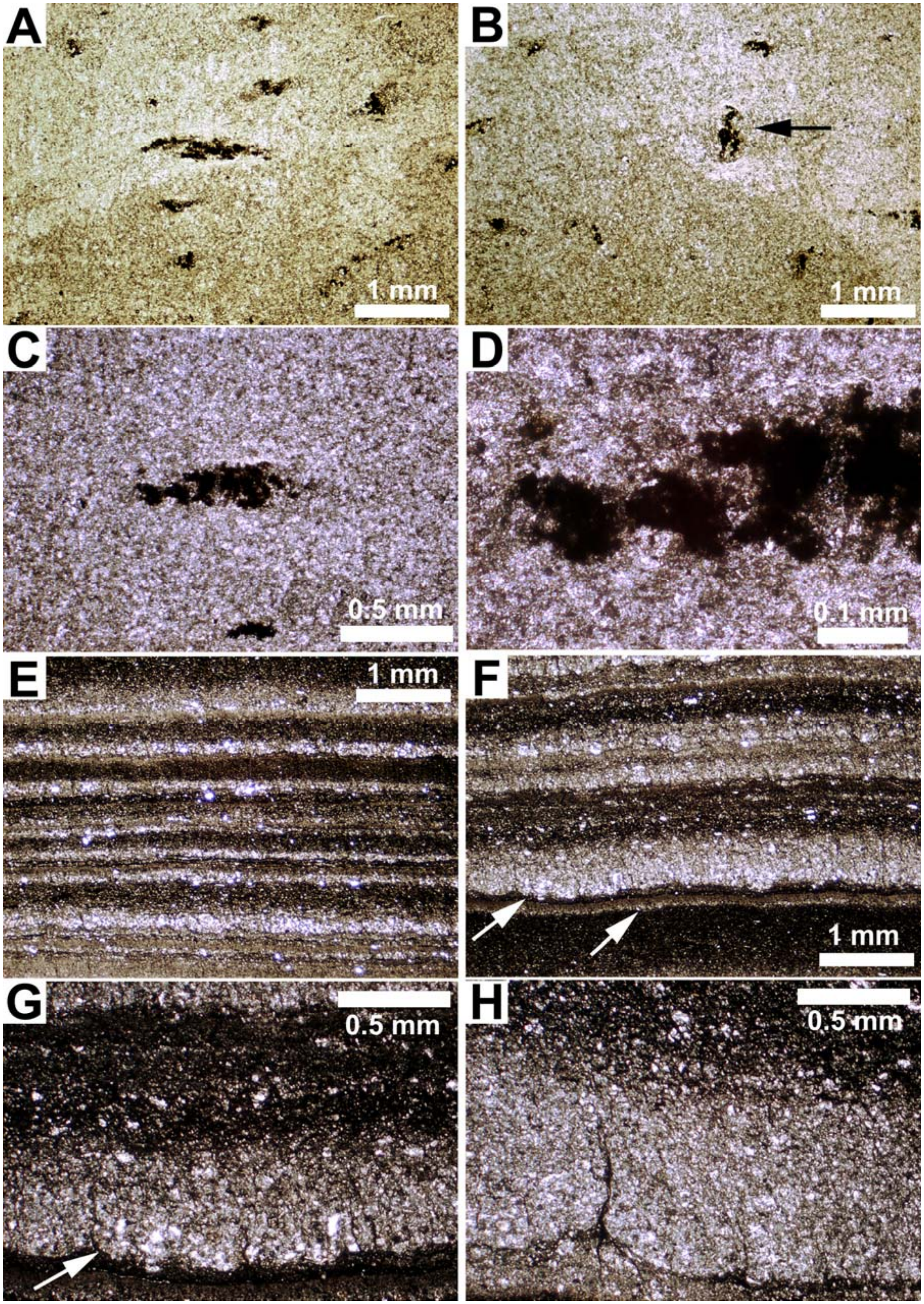

In: *Atlas of microbial mat features preserved within the clastic rock record*, Schieber, J., Bose, P.K., Eriksson, P.G., Banerjee, S., Sarkar, S., Altermann, W., and Catuneau, O., (Eds.), Elsevier, p. 171-180. (2007)

Fig. 7(c)-3 A - D: Lower portion of Tarur Nala Formation, photomicrographs of carbonaceous shales:

(A) Gray shale with carbonaceous lumps. These may be the degraded remains of microbial mat fragments that were transported into a deeper water setting. (B) In places these lumps show contortions (black arrow) that suggest shortening due to compaction of vertically embedded fragments of carbonaceous laminated shales. (C) & (D) Close-up views of carbonaceous lump in gray shale. Textural features of microbial mat laminae, such as seen in eroded mat fragments in Figures 8(c)-2 and 8(c)-4, are not visible.

Fig. 7(c)-3 E – H: Lower portion of Kopela Shale, photomicrographs of laminated silty shales:

(E) Photomicrograph of finely silt-laminated gray shale from the lower portion of the Kopela Shale. (F) Photomicrograph of finely silt-laminated gray shale from the lower portion of the Kopela Shale. Shows graded silt-mud couplets (lower white arrow), and graded silt layer with sharp base (upper white arrow). The irregular base of the latter layer is suggestive of scouring. (G) Close-up of graded silt layer with sharp, possibly micro-scoured base. (H) Close-up of graded silt layer with darker clay-rich tongues that extend upwards from the base. This may suggest that the irregular base may in part be due to formation of small load casts and the formation of complementary flame structures. However, caution needs to be exercised here because these rocks show in places a weakly developed slaty cleavage. Where this cleavage cuts across the base of graded layers it may produce features very similar to micro-scouring or tiny load and flame structures.

In: *Atlas of microbial mat features preserved within the clastic rock record*, Schieber, J., Bose, P.K., Eriksson, P.G., Banerjee, S., Sarkar, S., Altermann, W., and Catuneau, O., (Eds.), Elsevier, p. 171-180. (2007)

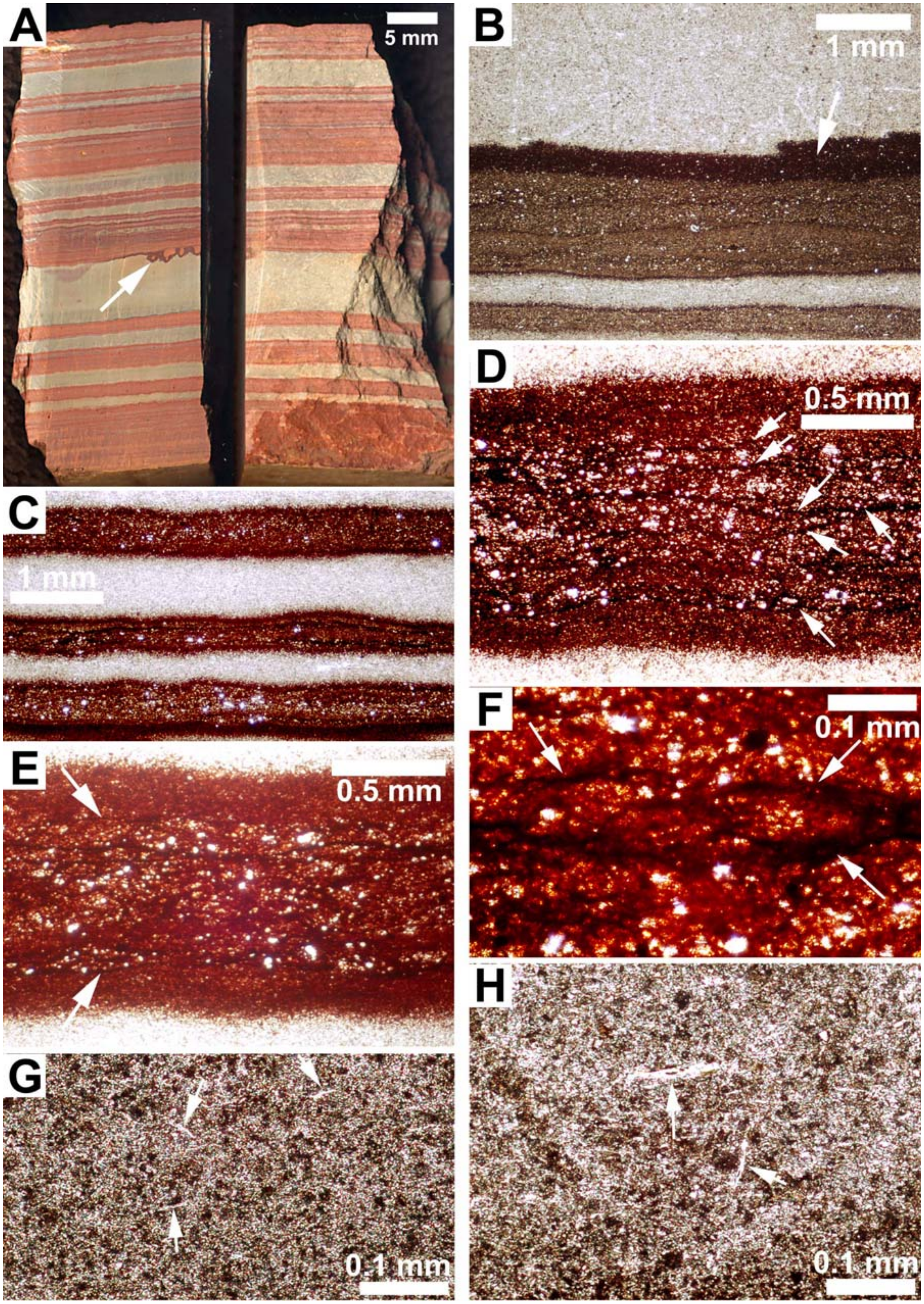

In: *Atlas of microbial mat features preserved within the clastic rock record*, Schieber, J., Bose, P.K., Eriksson, P.G., Banerjee, S., Sarkar, S., Altermann, W., and Catuneau, O., (Eds.), Elsevier, p. 171-180. (2007)

Figure 7(d)-4: Upper portion of Tarur Nala Formation, photos and photomicrographs of striped carbonaceous shales:

(A) Hand specimen photo of shale with alternating reddish and light buff layers. The red colour is due to oxidation. These specimens are texturally and compositionally very similar to strongly weathered striped shales from the Belt Basin (section 7(b)). We presume that beneath the zone of weathering, these shales will show alternating carbonaceous (wavy laminated and pyritic) and gray layers (mostly clay and silt), just like their textural counterparts in the Belt Basin (Schieber, 1986). During oxidation and pyrite destruction, dissolved iron migrated into the clay-dominated gray layers and locally caused cross-cutting impregnations with iron oxides (white arrow). (B) Photomicrograph (transmitted light) of thin section from same specimen as in (A). Shows that the darker (reddish-brown) layers are enriched in silt, and have wavy internal laminae. Also shows heavy iron oxide impregnation (white arrow) just above the silty and wavy laminated layer. (C) Photomicrograph of alternating dark (iron oxide-enriched) and light layers (clay-enriched). The darker iron-enriched layers have higher silt content, show wavy laminae, are iron oxide-enriched, and have diffuse iron oxide-enriched margins that fade into over- and underlying gray layers. (D) Close-up of dark (reddish) layer (photomicrograph, transmitted light). Shows wavy anastomosing laminae (arrows) and silt content. In striped shales of the Belt Basin (Schieber, 1986), the carbonaceous layers that are interpreted as microbial mat deposits are likewise enriched in silt and show wavy anastomosing internal laminae. In unweathered shale of this type (Belt Basin) the latter contain abundant organic matter and finely crystalline pyrite. (E) Another close-up (photomicrograph, transmitted light) of dark (reddish) layer with more abundant silt and wavy anastomosing laminae. White arrows point to upper and lower boundaries of the original carbonaceous and pyritic layer. The iron stained zones above and below the original layer represent weathering-related iron migration and impregnation. (F) Detail of anastomosing laminae (white arrows) seen in (D) and (E) (photomicrograph, transmitted light). (G) & (H) Detailed view of gray-buff interbeds as seen in (A) (photomicrograph, transmitted light). In comparison with (F) (taken at same magnification), the gray-buff layers are clearly lower in silt content. Large mica flakes are pointed out by white arrows. Note that the mica flakes are not aligned with bedding and may also be almost vertical (H). This suggests rapid deposition from a turbulent suspension. In the Belt Basin, analogous layers were interpreted as distal muddy tempestites.

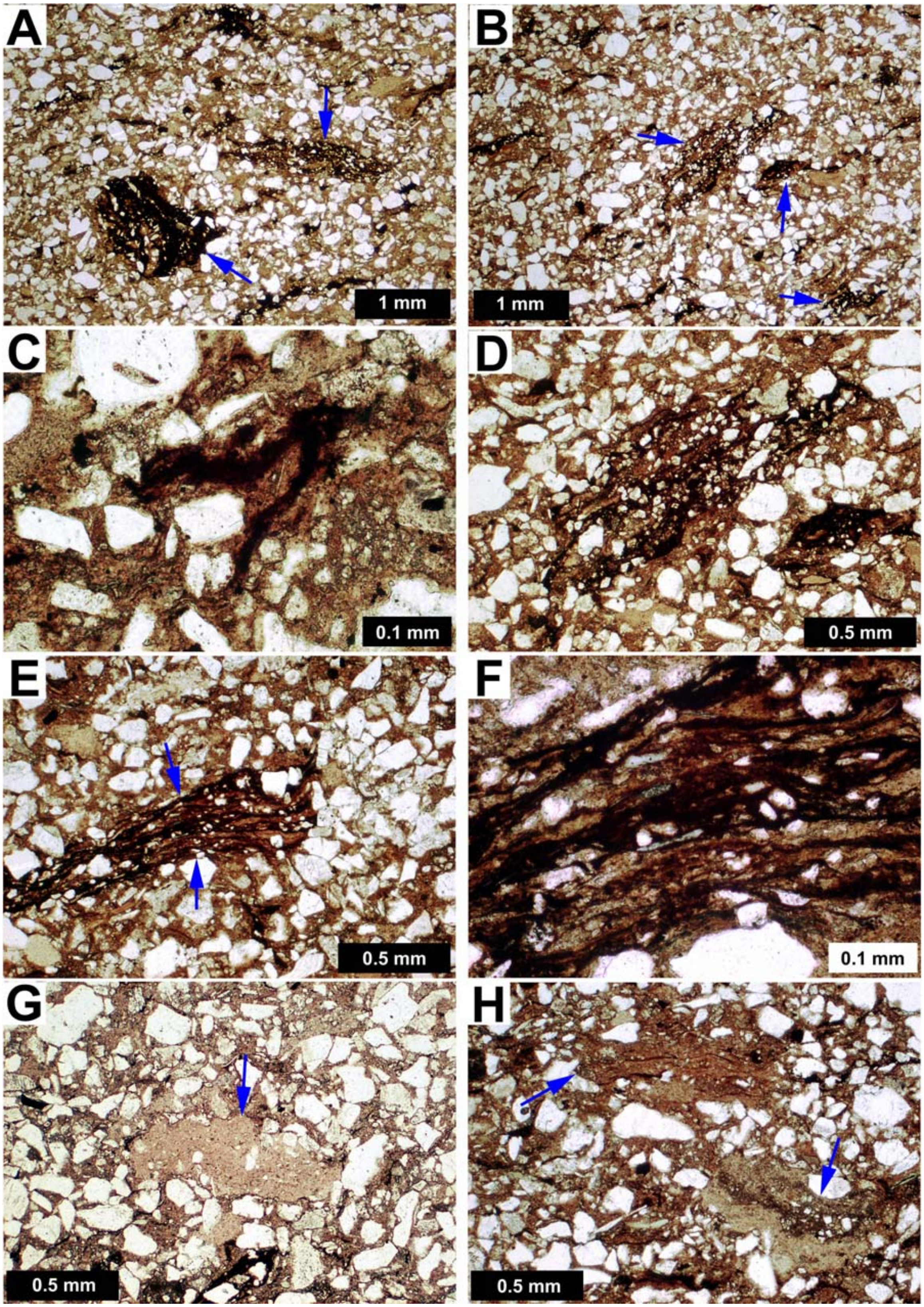

In: *Atlas of microbial mat features preserved within the clastic rock record*, Schieber, J., Bose, P.K., Eriksson, P.G., Banerjee, S., Sarkar, S., Altermann, W., and Catuneau, O., (Eds.), Elsevier, p. 171-180. (2007)

Figure 7(d)-5: Upper Portion of Tarur Nala Formation, photomicrographs from sandstone channel-fills within striped carbonaceous shales:

(A) & (B) Photomicrographs (transmitted light) of channel sandstone. These sandstones contain abundant shale clasts. Shale clasts are typically carbonaceous and have wavy-anastomosing internal laminae, and show soft sediment deformation (arrows). (C) Close-up photomicrograph (transmitted light) of strongly deformed small shale clast with a single carbonaceous lamina. (D) Close-up photomicrograph (transmitted light) of deformed shale clast seen in centre portion of (B). Note deformation and the much finer grain size (silt) that contrasts with the sand grains in the rock matrix. (E) & (F) Photomicrographs (transmitted light) of shale clast (arrows) with well developed wavy-anastomosing carbonaceous laminae (close-up in (F)). Note again the grain size contrast with the surrounding sand matrix, and the soft sediment deformation of the clast (see image (E)). (G) & (H) Close-up photomicrograph (transmitted light) of deformed shale clasts that lack carbonaceous laminae (arrows). These are clasts derived from other shale facies types that were laterally associated with the carbonaceous shales.

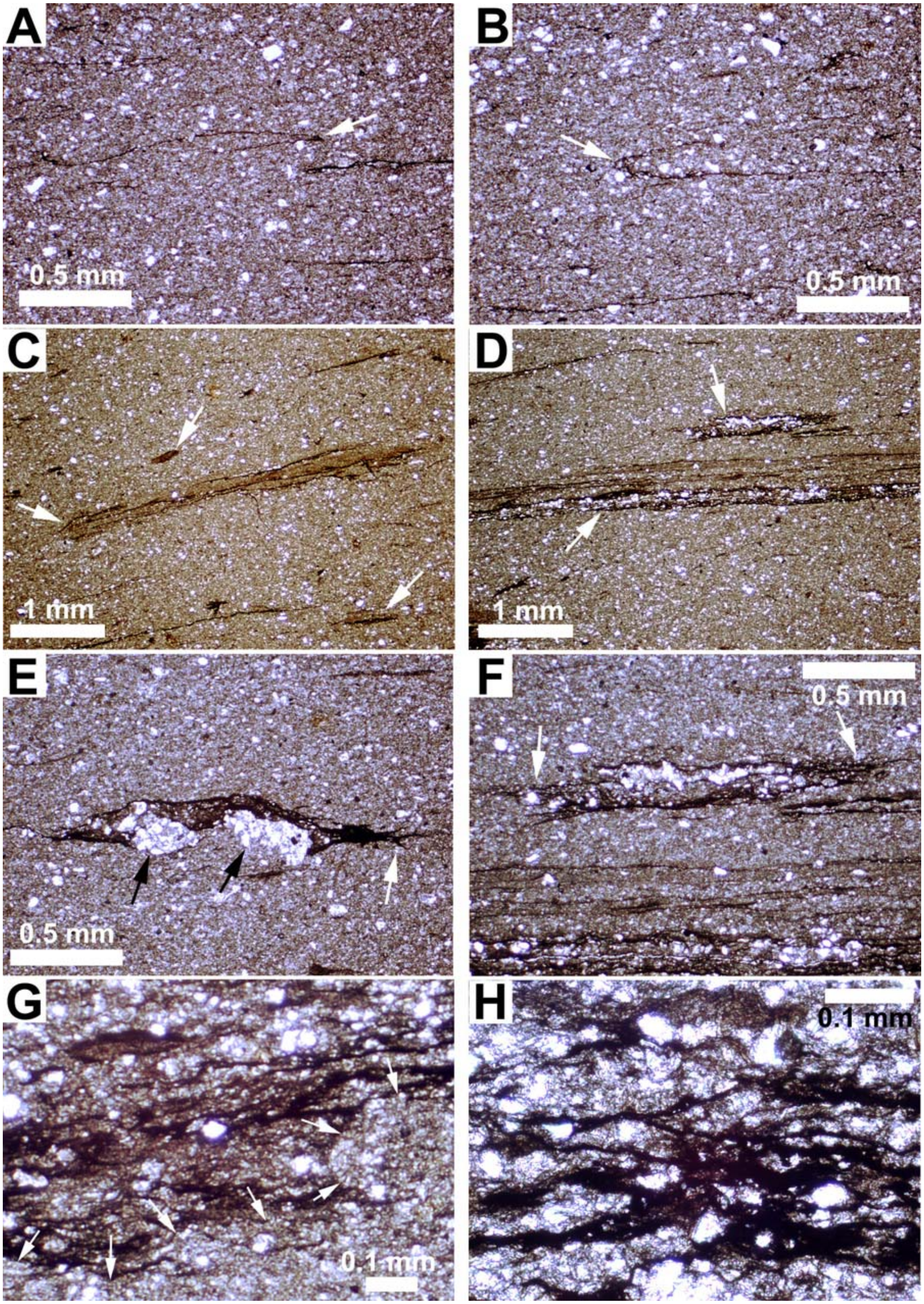

In: *Atlas of microbial mat features preserved within the clastic rock record*, Schieber, J., Bose, P.K., Eriksson, P.G., Banerjee, S., Sarkar, S., Altermann, W., and Catuneau, O., (Eds.), Elsevier, p. 171-180. (2007)

Figure 7(d)-6: Kopela Shale, photomicrographs of carbonaceous shales with microbial mat fragments:

(A)&(B) Gray shale with thin carbonaceous whisps. These very thin carbonaceous features show frequent occurrence of "fold-overs" (white arrows), an indication that they were thin, cohesive, sheet-like features at the time of deposition. (C) Carbonaceous whisps and larger shale clasts with internal carbonaceous laminae of the same appearance as carbonaceous whisps in (A) and (B). (D) More large shale clasts with internal carbonaceous laminae as in (C). These clasts also contain silt-rich carbonaceous laminae (white arrows). (E) Close-up of silty carbonaceous shale clast. Note deformation of shale clast around compaction-resistant "silt pockets" (black arrows) and wavy-anastomosing carbonaceous laminae. Also note the frayed character of carbonaceous laminae at right side of clast (white arrow). The more or less pure "silt pockets" associated with this fragment suggest that they adhered to the shale fragment during transport. Such adherence can be attributed to the binding properties of microbial slime (EPS) and/or microbial filaments, and the frayed edges attest to the tearing of a sheet-like material of comparatively high internal coherence. (F) Close-up of another silty carbonaceous shale clast. Note silt-rich lamina and frayed edges at either end of the clast (white arrows). The frayed character is accentuated by carbonaceous laminae and suggests that the cohesiveness of these clasts derives from the substance that formed the (now) carbonaceous laminae. These observations are consistent with a microbial mat origin for the carbonaceous laminae. (G): Frayed edge of carbonaceous silty shale clast in close-up. Note textural and compositional contrast between the clast and the surrounding matrix (lower right corner of image). Clast is higher in organic matter and silt-enriched, whereas surrounding shale matrix has more clay and less silt and organic matter. Contact between clast and shale matrix marked with white arrows. Close-up of texture of silty carbonaceous shale clast. Note anastomosing carbonaceous laminae and silt-rich lenses of clast..

References

Chaudhuri, A. K., D. Saha, G. K. Deb, S. Patranabis Deb, M. K. Mukherjee, and G. Ghosh. 2002. The Purana Basins of Southern Cratonic Province of India - A Case for Mesoproterozoic Fossil Rifts. Gondwana Research 5: 23-33.

Chaudhuri, Asru K., Joydip Mukhopadhyay, Sarbani Patranabis Deb, and S. K. Chanda. 1999. The Neoproterozoic cratonic successions of Peninsular India. Gondwana Research 2, 213-25.

Saha, D., Ghosh, G., 1998. Lithostratigraphy of deformed Proterozoic rocks from around the confluence of Godavari and Indravati rivers, South India. Indian Journal of Geology, v.70 (3), 217-230.

Schieber, J., 1985. The Relationship between Basin Evolution and Genesis of stratiform Sulfide Horizons in Mid-Proterozoic Sediments of Central Montana (Belt Supergroup), 811pp. Dissertation, University of Oregon.

Schieber, J., 1986. The possible role of benthic microbial mats during the formation of carbonaceous shales in shallow Proterozoic basins: Sedimentology, v. 33, p. 521-536.

Schieber, J., 1989. Facies and origin of shales from the Mid-Proterozoic Newland Formation, Belt basin, Montana, U.S.A.: Sedimentology, v. 36, p. 203-219.

Stow, D. A. V., and Shanmugam, G., 1980, Sequence of structures in fine-grained turbidites: Comparison of recent deep-sea and ancient flysch sediments: Sedimentary Geology, v. 25, pp. 23-42.

In: *Atlas of microbial mat features preserved within the clastic rock record*, Schieber, J., Bose, P.K., Eriksson, P.G., Banerjee, S., Sarkar, S., Altermann, W., and Catuneau, O., (Eds.), Elsevier, p. 171-180. (2007)